Annales Geophysicae (2004) 22: 985–992
SRef-ID: 1432-0576/ag/2004-22-985

Annales Geophysicae

The six-month line in geomagnetic long series

J. L. Le Mouël[1], E. Blanter[2], and M. Shnirman[2]

[1]Institut de Physique du Globe de Paris, 4, place Jussieu, Paris, Cedex 05, 75252 France
[2]International Institute of Earthquake Prediction Theory and Mathematical Geophysics, Warshavskoye shosse, 79, Korp 2, Moscow 113556, Russia

Received: 3 February 2003 – Revised: 24 July 2003 – Accepted: 5 August 2003 – Published: 19 March 2004

Abstract. Daily means of the horizontal components X (north) and Y (east) of the geomagnetic field are available in the form of long series (several tens of years). Nine observatories are used in the present study, whose series are among the longest. The amplitudes of the 6-month and 1-year periodic variations are estimated using a simple but original technique. A remarkably clear result emerges from the complexity of the geomagnetic data: the amplitude of the 6-month line presents, in all observatories, the same large variation (by a factor of 1.7) over the 1920–1990 time span, regular and quasi-sinusoidal. Nothing comparable comes out for the annual line. The 6-month line results from the modulation by an astronomical mechanism of a magnetospheric system of currents. As this latter mechanism is time invariant, the intensity of the system of currents itself must present the large variation observed on the 6-months variation amplitude. This variation presents some similarities with the one displayed by recent curves of reconstructed solar irradiance or the "Earth's temperature". Finally, the same analysis is applied to the *aa* magnetic index.

Key words. Geomagnetism and paleomagnetism (time variations, diurnal to secular). Magnetospheric physics (current systems; polar cap phenomena)

1 Introduction

Long series (several tens of years) of hourly and daily means of the components of the geomagnetic field are available from magnetic observatories. It has been known for a long time that a 1-year line and a 6-month line appear in the Fourier transform of the series (e.g. Currie, 1966; Courtillot and Le Mouël, 1976). Nevertheless, surprisingly enough, the geographical distribution of the amplitudes of these lines, not to speak of their phases, is very poorly known. For example, in induction studies, the 6-month variation is supposed to have the geometry of the field of an external axial dipole, i.e. a uniform field parallel to the rotation axis (Banks, 1969); this hypothesis is justified by an assumed ring current origin, but is rather arbitrary. Things are more complicated in the case of the annual line (Courtillot and Le Mouël, 1976; Runcorn and Winch, personal communication). Furthermore, to our knowledge, no study has ever been devoted to the possible variation in time of the amplitudes and possibly phases of these lines. These questions are addressed in the present paper.

Correspondence to: J. L. Le Mouël
(lemouel@ipgp.jussieu.fr)

2 A new analysis of the semiannual and annual lines

We consider here series of daily mean values of the north component (X) of the geomagnetic field from observatories whose names and locations are given in Table 1. Of course, we have tried to collect the longest and most continuous of these series, which does not mean that our list cannot be extended.

Direct analysis of the X series does not give reliable results. First, the 6-month and 12-month variations are superimposed on the powerful trend of the so-called secular variation of the main field of internal origin (which amounts to several tens, up to 80 nT per year), whereas their amplitude is only of the order of a few nT; some detrending is necessary. Second, some appropriate filtering of short time scale variations is also necessary. We adopted the following procedure which proved efficient. Let $X_i(k)$ be the time series of daily means of X at observatory O_i; k is the day number. The first step of the analysis consists of computing a running average of the series X defined by:

$$y_p(k) = \frac{1}{p} \sum_{j=-p+1}^{0} X(k+j).$$

With such a definition the running mean is computed backwards. In the following p is taken equal to 31. We use this first transformation to reduce the high frequency components. The second step consists of computing the slope of

Table 1. Names, acronyms and coordinates of magnetic observatories used in the study, and years available.

Name	Sigle	Geographical latitude	Geographical longitude	Geomagnetic latitude	Geomagnetic longitude	Years available
Chambon-la-Foret	CLF	48.02	2.26	43.36	79.32	1944–2000
Hartland	HAD	50.99	355.22	47.53	74.74	1926–2000
Eskdalemuir	ESK	55.30	356.80	52.15	76.30	1914–2000
Lerwick	LER	60.05	358.82	57.86	80.95	1926–2000
Sitka	SIT	57.07	224.67	59.71	280.30	1940–2000
Honolulu	HON	21.32	202.00	21.39	269.92	1940–2000
Hermanus	HER	−34.42	19.23	−42.43	82.62	1904–1976
Tucson	TUC	32.25	249.17	39.80	314.48	1914–1968
Kakioka	KAK	36.23	140.19	29.33	211.88	1925–2000

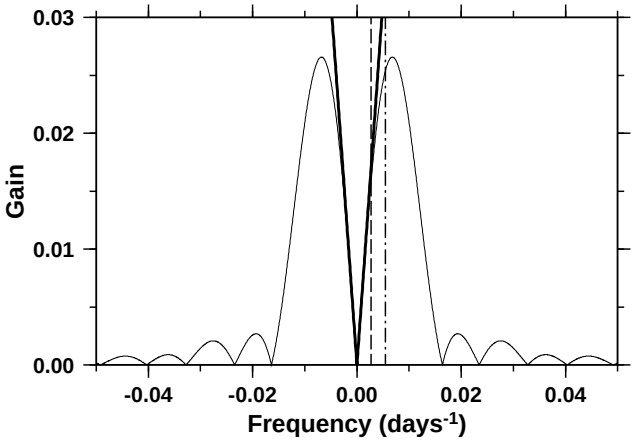

Fig. 1. Modulus of the transfer function $F(\upsilon)$ (Eq. (2) of main text), with p=61. The bold line represents the transfer function of the simple first derivative; the dashed line and the dashed-dotted line correspond to frequencies of, respectively, 1 year and 6 months.

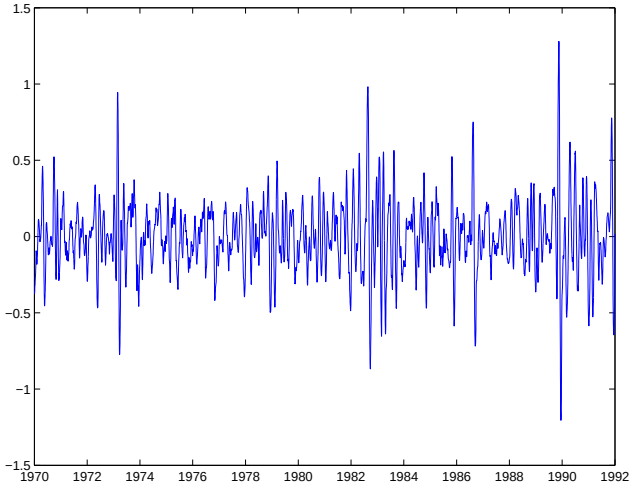

Fig. 2. HAD observatory. Function $\eta_p(k)$ (Eq. (1) of main text), with $p = 61$. Vertical unit : nT/day.

the linear regression of the so-obtained series $y_p(k)$ over a sliding window of length p,

$$\eta_p(i) = \frac{6}{p(p-1)}\left[\frac{2\sum_{j=-p+1}^{0}(j+p)y_p(i+j)}{p+1} - \sum_{j=-p+1}^{0} y_p(i+j)\right] . \quad (1)$$

As already noted, averages are computed backwards, so that the so-obtained filter is causal.

Let us denote $\hat{x}(\upsilon)$ and $\hat{\eta}(\upsilon)$, respectively, the Fourier transforms of the times series X and η, υ being the frequency; the transfer function $F(\upsilon)$ is defined such as $\hat{\eta}(\upsilon)=F(\upsilon)\hat{x}(\upsilon)$. Introducing $Z=\exp(-2i\pi\upsilon a)$, where a is the sampling interval, the transfer function of the linear filter described above is then,

$$F(Z) = \frac{6(1-Z^p)Z^{-p}}{p(p-1)(p+1)(1-Z)^3}$$

$$[2(1-Z^p) - 2pZ^{p-1}(1-Z) - (p+1)(1-Z)(1-Z^p)]. \quad (2)$$

The modulus of this complex function (also called the gain) is displayed in Fig. 1 for p equal to 61, that is 2 months for a sampling rate of 1 day.

As the filtering consists of taking the slope of the linear regression of the series over a window of length pa, it is equivalent, for a signal which evolves on time-scales much longer than pa, to taking the first derivative; we verify, Fig. 1, that the filter is indeed equivalent to a first derivative for frequencies lower than $1\,\mathrm{yr}^{-1}$ (long periods are attenuated by the derivation). For high frequencies (corresponding to periods shorter than 2 months), the gain of the filter is close to zero. This linear filter is thus a band-pass filter centered on a period of about 5 months.

An example of $\eta_p(k)$ is given in Fig. 2, over a 22-year time span (8035 days).

The transformed series $\eta_p(k)$ is then processed in the following way to extract the 6-month and 12-month lines. For day k, we consider the 22-year time interval centered at k and compute the 6-month and 12-month corresponding Fourier

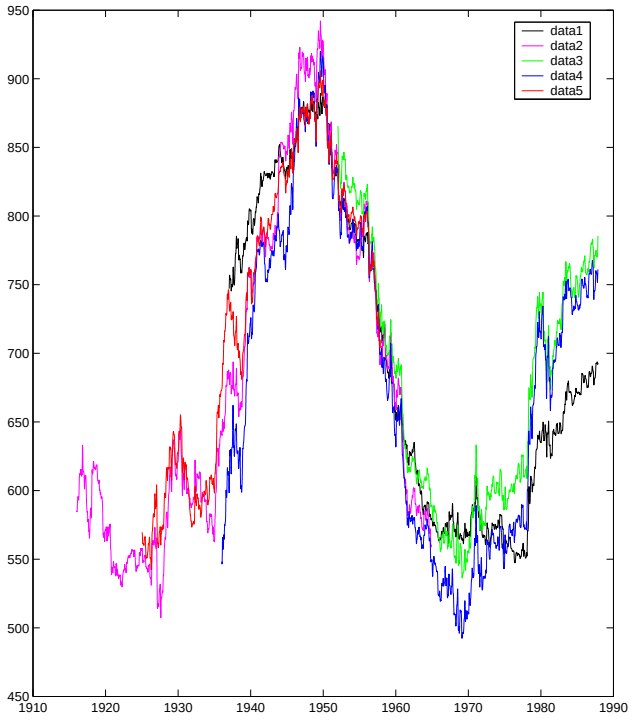

Fig. 3. Amplitude of the 6-month line, $A_6(t)$, for (1) LER (2) HER (3) HON(4) KAK (5) TUC. X component. Vertical unit: .35 10^{-3} nT/day.

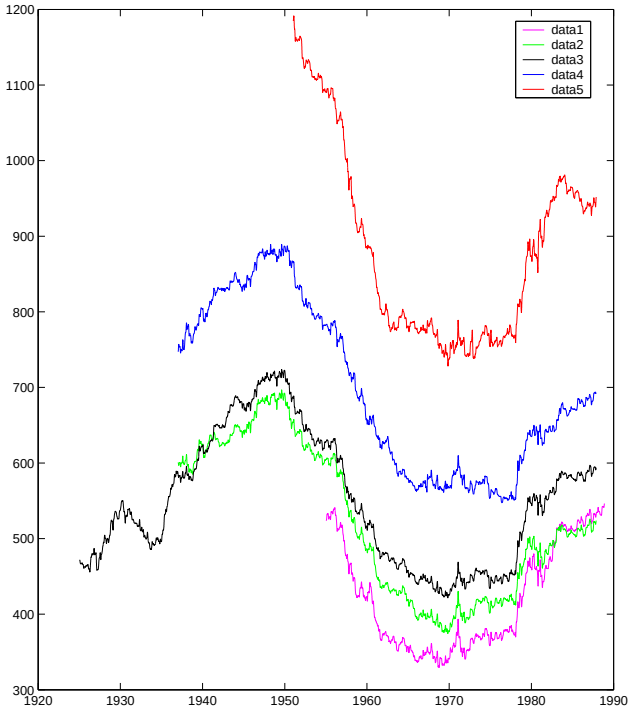

Fig. 4. Amplitude of the 6-months line, $A_6(t)$, for (1) CLF (2) HAD (3) ESK (4) LER (5) SIT. X component. Vertical unit: .35 10^{-3} nT/day.

coefficients:

$$\mathcal{A}_6(k) + i\mathcal{B}_6(k) = \frac{1}{2\tau+1} \sum_{p=k-\tau}^{k+\tau} \eta_p(\rho) \left(\cos \frac{2\pi}{T_6}\rho + \mathrm{isin}\frac{2\pi}{T_6} \right)$$

with $2\tau+1$=8035, T_6=182.62; and the same for $\mathcal{A}_{12}$ and $\mathcal{B}_{12}$ with T_{12}=365.25. The amplitude of the corresponding line is:

$$A_6(k) = \left(\mathcal{A}_6^2(k) + \mathcal{B}_6^2(k) \right)^{1/2}.$$

The same for $A_{12}(k)$. We will now present the results relative to A_6 and $A_{12}(k)$.

3 The 6-month line

Figures 3 and 4 show the time variation of $A_6(k)$ for different observatories (remember that there is an estimate of $A_6(k)$ per day, and that the lengths of the series depend on the observatory; see Table 1). In Fig. 3 we present the graphs of HER, HON, KAK, LER, TUC (see Table 1 and map of Fig. 5), five observatories which are far away from each other, with series of comparable lengths. The general shape of the graph is strikingly the same in all observatories; furthermore, many short features (a few years time scale) can be retrieved on the 5 graphs. The amplitude of the observed 50-year oscillation (we will call this observed quasi-sinusoidal variation an oscillation; we do not pretend that periodicity extends outside the observation time span) is by no means small: the amplitude of the 6-month line, in all the observatories, varies by a factor of 1.70. Figure 4 displays the graphs relative to European observatories (CLF, HAD, ESK, LER), and SIT (see again Table 1 and map of Fig. 5). Again, the similarity of graphs is striking, and many short time scale features are common to the five of them. Similarity with the graphs of Fig. 3a is made clear by the presence of LER graph in both figures.

The remarkable stability of the estimate of the 6-month line from an observatory to another gives us confidence in the physical significance and the value of this estimate. Tests of this significance can be made directly from the theory of Sect. 3; it is simple arithmetic. $\mathcal{A}_6$ and $\mathcal{B}_6$ are indeed simply Fourier coefficients of the 22-year long series $X(t)$, an example of which is given in Fig. 2. We are considering here an astronomical sharp line, not some peak in a spectrum. This is illustrated by Fig. 6, which shows how the figure of $A_6(t)$ and its amplitude change when varying T_6 around 182.6 days in Eq. (2). Maybe some sharper estimate of T_6 would be expected; but the time span used to compute $\mathcal{A}_6+i\mathcal{B}_6$ is rather short, and the amplitude of the 6-month variation is not constant over it.

3.1 The geometry of the 6-month line

In most studies of the geometry – distribution at the Earth's surface of the 6-month line's amplitude and phase, generally aimed at the global Earth induction problem, it is assumed

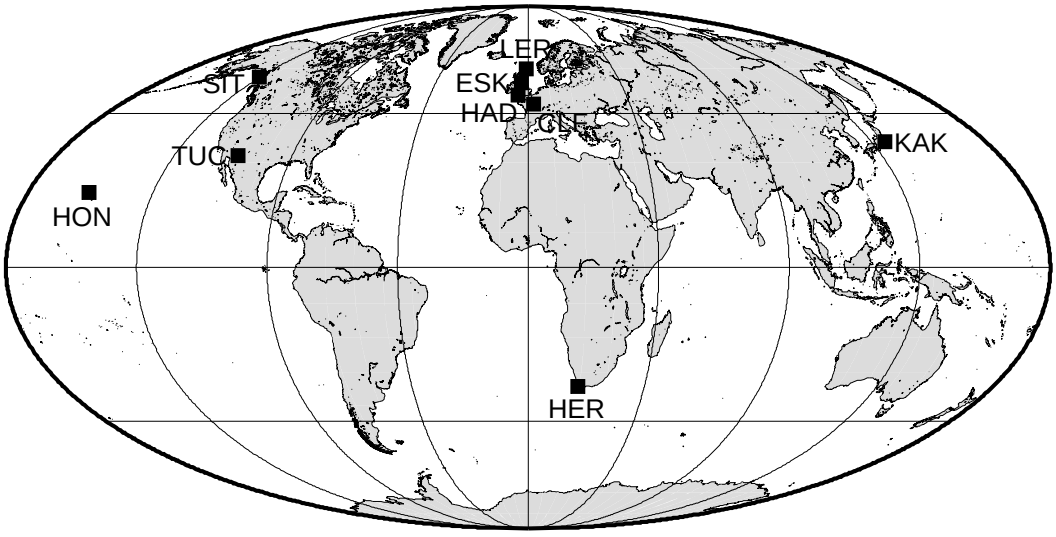

Fig. 5. Map of the observatories included in the study.

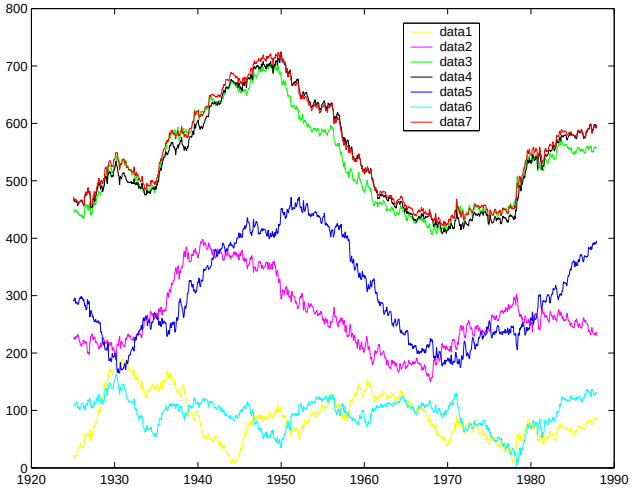

Fig. 6. Variation of the amplitude of the 6-month line, $A_6(t)$, when varying the period T_6 around 182,6 days. Vertical unit: .35 10^{-3} nT/day. (1) T_6=178; (2) T_6=180; (3) T_6=182; (4) T_6=183; (5) T_6=185; (6) T_6=187; (7) T_6=182.62.

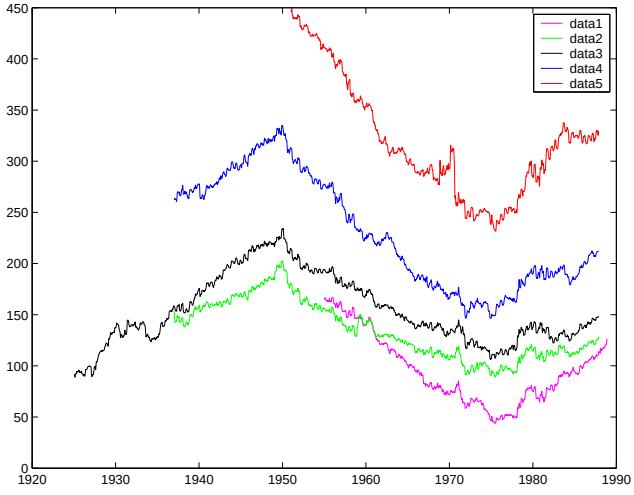

Fig. 7. Amplitude of the 6-month line, $A_6(t)$, for (1) CLF (2) HAD (3) ESK (4) LER (5) SIT. Y (east) component. Vertical unit: .35 10^{-3} nT/day.

that the geometry of A_6 is characterized by a P_1^O term (Banks, 1969; Courtillot and Le Mouël, 1976). The Dst field, which is supposed to generate the semiannual line, is indeed schematised as an approximately uniform axial field in the neighbourhood of the Earth (more exactly, the field of an equatorial ring current with a radius of a few Earth radii: see Daglis et al. (1999) and Søraas et al. (2002) for a modern description of the ring current). Clearly, this is not true; Dst is not alone in the generation of the 6-month line.

The variation of A_6 with latitude (or the ratios $A_6(O_i)/A_6(O_j)$, O_i and O_j being two observatories of latitudes L_i and L_j) is not exactly constant in time. But, neglecting it for the moment, it can be grossly said that the amplitude of the 6-month line is approximately the same in the 4 low-latitude observatories (HON, TUC, KAK, HER), smaller in the mid-latitude observatories (CLF, HAD, ESK), larger again in observatories of higher latitude (LER), and "abnormally" high at SIT (in the sense that latitudes – and also geomagnetic latitudes – of LER and SIT are quite close to one another). The geometry of the A_6 line amplitude cannot be better described with only this small number of stations. Therefore, more observatories are necessary.

Up to now we have considered only the X (north) component. It was generally considered that the 6-month variation was "small" on the Y (east) component, which is not true. The analysis can easily be extended to Y. Figure 7 is to be compared with Fig. 4. Clearly, the 6-month line amplitudes present the same gross trend for X and Y. The analysis

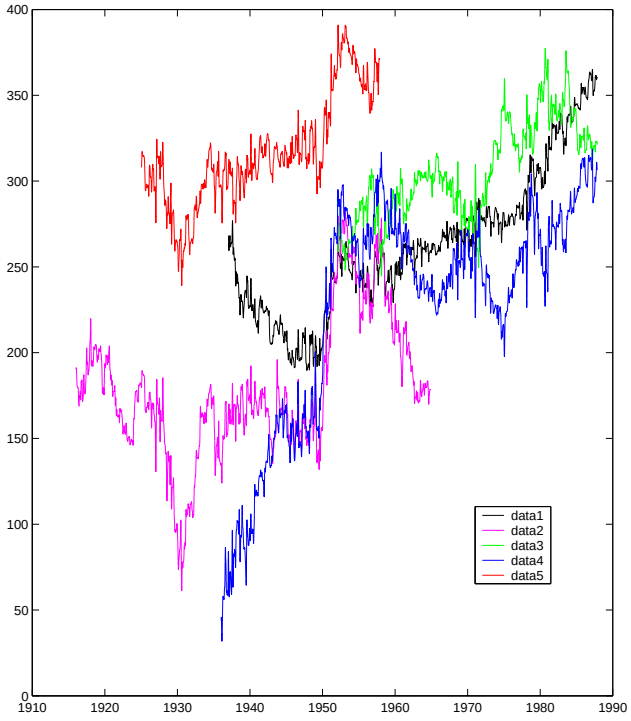

Fig. 8. Amplitude of the 12-month line, $A_{12}(t)$, for (1) LER (2) HER (3) HON (4) KAK (5) TUC. X component. Vertical unit: .35 10^{-3} nT/day.

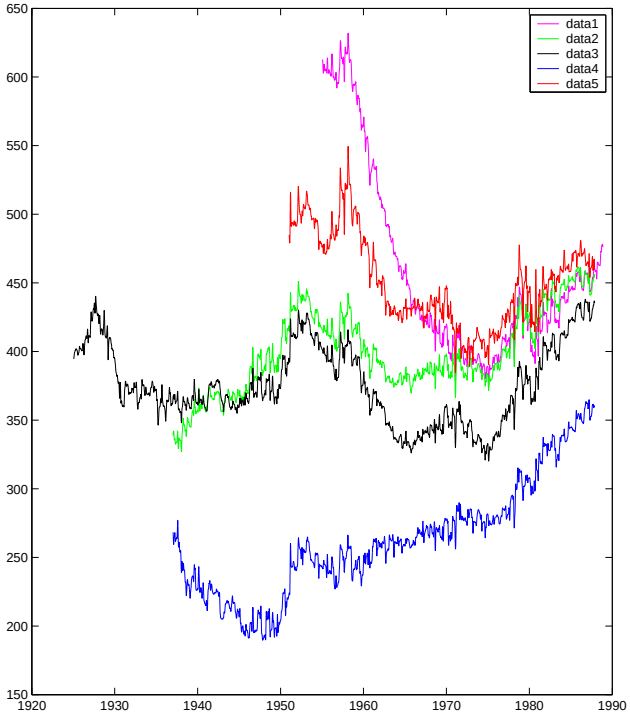

Fig. 9. Amplitude of the 12-month line, $A_{12}(t)$, for (1) CLF (2) HAD (3) ESK(4) LER (5) SIT. Vertical unit: .35 10^{-3} nT/day.

of long series of Z (vertical) values gives results which are much less clear. This is essentially – but probably not totally – due to defects in the ancient Z variometers (made of a poorly temperature corrected or/and unstable balance magnet); things are of course different for recent times.

3.2 Time variation of the system of currents responsible for the 6-months line

We will limit ourselves to a qualitative discussion of the above results. The transient variations of the external geomagnetic field $\boldsymbol{B}_e$ can be classified as regular and irregular (Mayaud, 1978). The regular variations are due to permanent sources of field which cause the daily occurrence of a certain variation during certain local times at a given point on the Earth; the irregular variations are generated by sources which do not permanently exist and, hence, their occurrence is basically sporadic. Let us write:

$$\boldsymbol{B}_e(\boldsymbol{r}, t) = \boldsymbol{S}_R(\boldsymbol{r}, t) + \boldsymbol{D}(\boldsymbol{r}, t),$$

$\boldsymbol{r}$ where is the position vector, t is time. $\boldsymbol{S}_R$ is for the regular field, $\boldsymbol{D}$ for the irregular one (disturbance).

Let us first consider the solar daily variation $\boldsymbol{S}_R$. We use here daily averages; the daily average of the east component of $\boldsymbol{S}_R$ is zero (not the X one). Figure 7 shows that Y displays a 6-month line. Furthermore, $\boldsymbol{S}_R$ is expected to present an annual variation, not a semiannual one. We can safely discard the $\boldsymbol{S}_R$ current system as a source of the 6-month line.

The disturbance field $\boldsymbol{D}$, following Fukushima and Kamide (1973) can be written:

$$\boldsymbol{D} = \boldsymbol{D}_R + \boldsymbol{D}_P + (\boldsymbol{D}_{CF} + \boldsymbol{D}_T).$$

$\boldsymbol{D}_R$ was thought to be the disturbance field generated by a single ring current in the geomagnetic equatorial plane, with a radius of several Earth radii; it has been shown, however, that there is not a "ring current", but rather several partial rings that feed field-aligned currents to and from the magnetosphere (Campbell, 1996). $\boldsymbol{D}_P$ is the geomagnetic disturbance field caused primarily by intense electrojets flowing in the ionosphere of the polar region (including the auroral zone) and their accompanying currents in the ionosphere or magnetosphere, or both. $\boldsymbol{D}_{CF}$ and $\boldsymbol{D}_T$ fields can generally be neglected at the Earth's surface.

The observed geographical distribution of the 6-month line (Figs. 3 and 4) shows that it cannot be explained by the ring current alone (there is an enhancement of the line amplitude at high latitudes). It can be concluded that the systems of currents responsible for the semiannual variation are both $\boldsymbol{D}_R$ and $\boldsymbol{D}_P$ (the electrojets give a systematically negative contribution to the X component at the considered observatories), i.e. the ring current system and the auroral electrojets. Again, let us call $\boldsymbol{D}$ the sum of the two.

The existence of the 6-month line shows that $\boldsymbol{D}$ is (weakly) modulated at this period. The mechanism of this modulation is presumably the change in the Earth's axis inclination on the Earth-Sun line, or solar wind direction, through

Fig. 10. Amplitude of the 6-month line (1) X component, HAD observatory (2) aa index. Vertical unit: .35 10^{-3} nT/day. Right vertical scale is for aa.

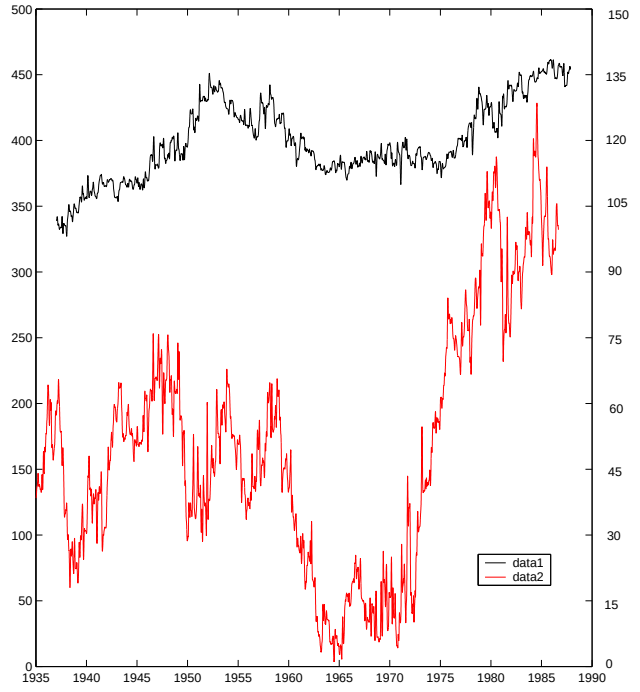

Fig. 11. Amplitude of the 12-month line (1) X component, HAD observatory (2) aa index. Vertical unit: .35 10^{-3} nT/day. Right vertical scale is for aa.

the correlated change in the average dipole axis inclination (Russel-Mc Pherron effect). There has been, of course, no change in this astronomical phenomenon during a 100-years time span. Therefore, the system of currents which generates the 6-month line through the Russel-Mc Pherron effect presents itself the oscillation illustrated by Figs. 3 and 4. The semi-annual variation presents the same phase all over the Earth, and its amplitude presents the same decade variations in the ten observatories of this study (representative curves are similar, or affine one to the other; Figs. 3, 4, and 7). Therefore, the modulation of the system of currents generating the 6-month line can be written:

$$D_6(\boldsymbol{r}, t) = d(\boldsymbol{r}) \cos 2\pi (t/T_6) D_6(t),$$

where T_6=6 months; $D_6(t)$ is a scalar function, the shape of which is illustrated by Figs. 3, 4, and 7; a convenient origin of time is chosen.

3.3 Discussion

Is there any indication of a time variation similar to $D_6(t)$ in other magnetic parameters or, better yet, in solar data? Total solar irradiance has been measured only since 1978, using radiometers aboard spacecrafts. Reconstructions of solar irradiance have been made recently (Lockwood et al., 1999; Solanki et al., 2000) using the 140-year long aa geomagnetic index series (Mayaud, 1972). The reconstructed solar irradiance curve presents a maximum around 1960, a minimum around 1970, then increases again, just as the $D_6(t)$ curve does (the irradiance curve of Solanki is made of 11-year running averages). In fact, it is enough to take the aa series itself, as it is, and compute 22-year running means $\overline{aa}$ (recall that estimates $A_6(t)$ (Sect. 2) are representative of 22-year time intervals centered on t) to obtain a similar behaviour (although less regular than the D_6 one). More generally, as will be shown in a next paper, the oscillation displayed by $\overline{aa}$ over the last 70 years is also conspicuous on the representative curves of all the parameters which can be derived from magnetic observatories. It is also conspicuous on the Wolf number series.

Solanki (2002) compares the reconstructed solar irradiance with the so-called Earth's temperature (the global temperature derived from numerous climatological records) and observes that "obviously, prior roughly to 1980, the solar irradiance in the whole ran parallel to and even slightly ahead of the Earth's temperature". Comparing the $\overline{aa}$ curve with the same Earth's temperature leads to the same conclusion (except that it is hazardous to state that $\overline{aa}$ leads temperature). In any case, it seems that the possible relationship between solar activity and the Earth's climate deserves serious consideration (the first encouraging result is probably the correlation between the length of the sunspot number and the Northern Hemisphere's air temperature, suggested by Friiss-Christensen and Lassen, 1991).

4 The annual line

We also considered the 12-month line in the Fourier content of the time variation of the geomagnetic field; the results are quite different. Figures 8 and 9 are, respectively, analog, for the annual line, to Figs. 3 and 4. It appears that the curves corresponding to the different observatories are less similar, except for the group made of the European observatories (HAD, ESK, LER), relatively close to one another, and SIT, and the couple TUC-HON. The annual line has long been attributed to systems of currents different from the ones responsible for the semiannual line (e.g. a modulation of the ionospheric dynamo mechanism, Currie 1966). In fact, the geometry of the annual line, although poorly sketched in former studies, appears so difficult to account for by ionospheric or magnetospheric sources that some authors (Runcorn and Winch, personal communication) attributed it to motions of the conductive water of the ocean in the Earth's main field. It might also be tempting to attribute the intricate time variations of the annual line amplitude to instrumental effects (essentially temperature effects on the magnets of the variometers). But this is dubious. It could be the case for the Z component (discarded here), at least before the introduction of fluxgate sensors in the seventies. But the temperature effect was much easier to correct for the horizontal ($\sim X$) component, and is quite small, in most places, for Y (the declination variometer is not sensitive to temperature). Furthermore, there is enough correlation between some of the curves to discard this interpretation.

5 The *aa* index

The *aa* index is a measure of geomagnetic activity, and is considered as a proxy of solar activity (we repeat that total Sun irradiance has been recently reconstructed from the *aa* series). Let us apply exactly the same procedure as before to the series of daily averages of *aa* index (*aa* for a given day is the average of the 8 tri-hourly indices of the day). Results are illustrated by Figs. 10 and 11 which display the time variation of, respectively, the 6-month and the annual line's amplitudes beside the corresponding HAD curves (already shown in Figs. 4 and 9). Units are the same for *aa* and X (HAD) since *aa* is expressed in nT. It is seen that $\alpha_6(aa)$, the amplitude of the semiannual line of *aa* index, follows rather well A_6 (HAD) from 1935 to around 1978, then suddenly decreases instead of increasing like A_6 (HAD) (all the A_6 (O_i) increased after 1975). We have no interpretation of this unexpected behaviour at the present time, but will try to understand what its origin might be (either a computation artifact or a genuine – small – change in the distribution of magnetic activity).

The discrepancy after 1978 comes from taking an erroneous data file. When taking the correct one, a quasi perfect fit is observed over the whole time span, as conjectured by one of the referees.

Let us emphasize again that the amplitude α_6 changes greatly, by a factor of 2.5. The amplitude of the annual line of aa, α_{12}, is much smaller than the one of the 6-month line, varying between 0 in the 1965–1970 time interval and 120 in 1990 (Fig. 11).

6 Conclusion and perspectives

Our main result is the following: the amplitude A_6 (t, O_i) of the 6-month line in the derivative of the series of daily averages computed, after a proper filtering, on 22-year interval centred on the current day t, displays in all observatories O_i, a similar oscillation; this oscillation presents, in the longest time interval covered by the observations, the form of a sine wave with a period of about 50 years (again, we do not claim that this wave repeats itself outside this interval). Nothing comparable is observed for the annual line. The modulation of the 6-month line amplitude is attributed to a corresponding modulation of the current system responsible for it (the so-called ring current field and the auroral electrojets). This modulation must, in turn, in some way be attributed to some change in the solar activity. Some similarity can be found between our $A_6(t)$ curves and the variation of the temperature of the Earth (see the relevant quoted papers for a definition of this temperature), as well as with the reconstructed total solar irradiance (the latter two parameters are shown to "run parallel on the whole"; Solanki, 2002). In fact, all the parameters representative of the intensity of the magnetic variations (not only of the so-called disturbance activity) appear to present a similar variation over the latter hundred years. This will be the subject of our next study.

Acknowledgements. We thank P. N. Mayaud and R. Hide for fruitful discussions, and all the observatories for providing us with the series.

We thank two anonymous referees for valuable comments.

The Editor in Chief thanks I. A. Daglis and E. Cliver for their help in evaluating this paper.

References

Banks, R. J.: Geomagnetical variations and the electrical conductivity of the upper mantle, Geophys. J. Roy. Astron. Soc., 17, 457–487, 1969.

Campbell, W. H.: Dst is not a pure ring-current index, EOS Trans. AGU, 77, 30, 283–285, 1996.

Courtillot, V. and Le Mouël, J.-L.: On the long-period variations of the earth's magnetic field from 2 months to 20 years, AGU, 81, 17, 2941–2950, 1976.

Currie, R.: The geomagnetic spectrum-40 days to 5.5 years, J. Geophys. Res., 71, 4579–4598, 1966.

Daglis, I., Thorne, R., Baumjohann, W., and Orsini, S.: The terrestrial ring current: origin, formation, and decay, AGU, 37, 4, 407–438, 1999.

Friiss-Christensen, E. and Lassen, K.: Length of the solar cycle: an indicator of solar activity closely associated with climate, Science, 254, 698–700, 1991.

Fukushima, N. and Kamide, Y.: Partial ring current models for worldwide geomagnetic disturbances, Rev. Geophys. Space Phys., 11, 795–853, 1973.

Lockwood, M., Stamper, R., and Wild, M.: A doubling of the sun's coronal magnetic field during he past 100 years, Nature, 399, 437–439, 1999.

Mayaud, P.: Derivation, Meaning, and Use of Geomagnetic Indices, Geophysical monograph, AGU, Wash. D. C., 1980.

Mayaud, P.: Morphology of the transient irregular variations of the terrestrial magnetic field, and their main statistical laws, Ann. Géophys., 34, 243, 1978.

Mayaud, P.: The *aa* indices : A 100-year series characterizing the magnetic activity, J. Geophys. Res., 77, 6870, 1972.

Solanki, S.: Solar variability and climate change: is there a link? Astronomy and geophysics, 43, 5.9–5.13, 2002.

Solanki, S. and Schüsser, M.: Evolution of the sun's large scale magnetic field since the maunder minimum, Nature, 408, 445–447, 2000.

Søraas, F., Aarnes, K., Oksavik, K., and Evans, D.: Ring current intensity estimated from low-altitude proton observations, J. Geophys. Research, 107, 1–10, 2002.